KAWASAKI STEEL TECHNICAL REPORT
No.9 (March 1984)

Control of Strip Buckling and Snaking in Continuous Annealing Furnace

Tohru Sasaki, Takaaki Hira, Hideo Abe, Fumiya Yanagishima, Yuji Shimoyama, Kohichi Tahara

Synopsis :
The mechanism of buckling and snaking that sometimes occur in a strip traveling through the heating and soaking zones of a continuous annealing furnace was made clear by conducting stress analysis by the finite element method (FEM), a simulation test using aluminum foil and experiments in a commercial-scale continuous annealing line. Measures to prevent strip buckling and snaking were contrived based on the results of these tests. Although the crown of the hearth roll has the function of correcting the snaking of the strip, it gives nonuniform tension to the strip, thereby generating compressive membrane stresses in the strip which comes to buckle. The larger the strip width and the smaller the width of the parallel cylindrical part of the hearth roll, the more the strip will be apt to buckle. to prevent buckling and snaking simultaneously, it is effective to install auxiliary rolls, for example, to near the hearth roll and thereby flatten the profile of the strip.

The body can be viewed from the next page.

Control of Strip Buckling and Snaking in Continuous Annealing Furnace*

Tohru SASAKI** Takaaki HIRA** Hideo ABE**
Fumiya YANAGISHIMA*** Yuji SHIMOYAMA*** Kohichi TAHARA****

The mechanism of buckling and snaking that sometimes occur in a strip traveling through the heating and soaking zones of a continuous annealing furnace was made clear by conducting stress analysis by the finite element method (FEM), a simulation test using aluminum foil and experiments in a commercial-scale continuous annealing line. Measures to prevent strip buckling and snaking were contrived based on the results of these tests. Although the crown of the hearth roll has the function of correcting the snaking of the strip, it gives nonuniform tension to the strip, thereby generating compressive membrane stresses in the strip which comes to buckle. The larger the strip width and the smaller the width of the parallel cylindrical part of the hearth roll, the more the strip will be apt to buckle. To prevent buckling and snaking simultaneously, it is effective to install auxiliary rolls, for example, to near the hearth roll and thereby flatten the profile of the strip.

1 Introduction

Crowns of various profiles are given to hearth rolls in a continuous annealing furnace for the purpose of preventing strip snaking. However, these crowns generate nonuniform tension in the strip, which generates compressive membrane stresses. When the strip width is large and the annealing temperature is high at the same time, these compressive membrane stresses in the strip may exceed the critical buckling stress thus resulting in buckling in the width direction of the strip (hereinafter called heat buckling). It is known that heat buckling is apt to occur in the heating and soaking zones and that with the same type of strip, the higher the tension during the travel of the strip, the more this phenomenon will be apt to take place[1]. However, if this tension is lowered, the strip snakes in the width direction[2]. Therefore, it is necessary to cause the strip to travel in the furnace under such optimum tension range as will fit to strip size, chemical composition of steel and annealing temperature so as to prevent snaking or heat buckling. It is known by experience that in ultralow carbon steel strip of 0.002%C and under, and 1 300 mm and over in width, heat buckling tends to occur because of their very narrow optimum tension range.

The mechanism of heat buckling and snaking of the strip was made clear by conducting a simulation test using aluminum foil, stress analysis by the finite element method and experiments in a commercial-scale continuous annealing line. This report presents an outline of the results obtained and touches upon measures for preventing heat buckling and snaking.

2 Experimental Method

To simulate heat buckling, the experimental equipment shown in **Fig. 1** was fabricated in 1/5 of an actual commercial-scale equipment size, and a simulation test[3] was conducted by using aluminum foil. In this figure, only roll B is driven and the maximum peripheral speed of this roll is 7.5 m/min. The tension of the material was controlled by a counterweight placed on roll E. Crowns of various profiles were given to roll A only and all other rolls were flat cylindrical rolls. In this arrangement, an investigation was made into the effect of the profile of roll A on the buckling behavior. The existence or nonexistence of buckling was judged by rule of thumb.

* Originally published in *Kawasaki Steel Giho*, **16** (1984) 1, pp. 37–45
** Research Laboratories
*** Chiba Works
**** Hanshin Works

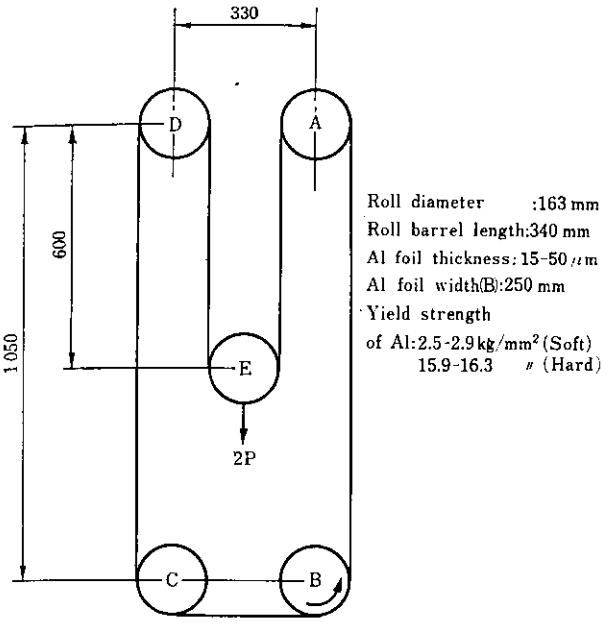

Fig. 1 Arrangement of experimental equipment

Furthermore, to investigate the relationship between the shifting condition of the strip in the width direction and the roll profile during the strip travel, a rubber band was wound on rolls A and B of this experimental equipment and the number of roll rotation and the amount of shift of the material in the width direction were measured. The sizes of the rolls and material are shown in the figure.

3 Heat Buckling Simulation Using Aluminum Foil

3.1 Type of Heat Buckling

Photo 1 shows appearances of buckled aluminum foil in the simulation test. These appearances are very similar to those observed in a commercial line, and vary depending on the roll profile. In this photo, the type (1) occurred when a roll with rectilinearly tapered ends (hereinafter called a tapered roll) was used. It is apparent that buckling took place at the shoulders of the tapers. The type (2) occurred when a roll with crowns of circular profile (hereinafter called a round roll) was used. In this case, buckling is apt to take place in the middle of the width. The type (3) is a buckling phenomenon that occurs aslant due to the shearing force generated when the material snakes. This type of buckling occurs also in flat rolls without crown. The types (1) and (2) are often observed in a commercial line in wide strip of low strength, and the type (3) in narrow strip such as those for tinplate.

An investigation was made as to whether the material buckles or not when it is caused to travel round by driving roll B in the experimental equipment shown in Fig. 1. **Figure 2** shows the relationship between the amount of roll taper and tension and the occurrence of buckling. The material thickness (t) is 15, 20, 30 and 50 μm. Fully-annealed aluminum foil with yield strength (Y.S.) of 2.5 to 2.9 kgf/mm² and temper-rolled aluminum foil with Y.S. of 16 kgf/mm² were used with t of 20 μm. Only fully-annealed aluminum foil was used for other thicknesses. Tapered

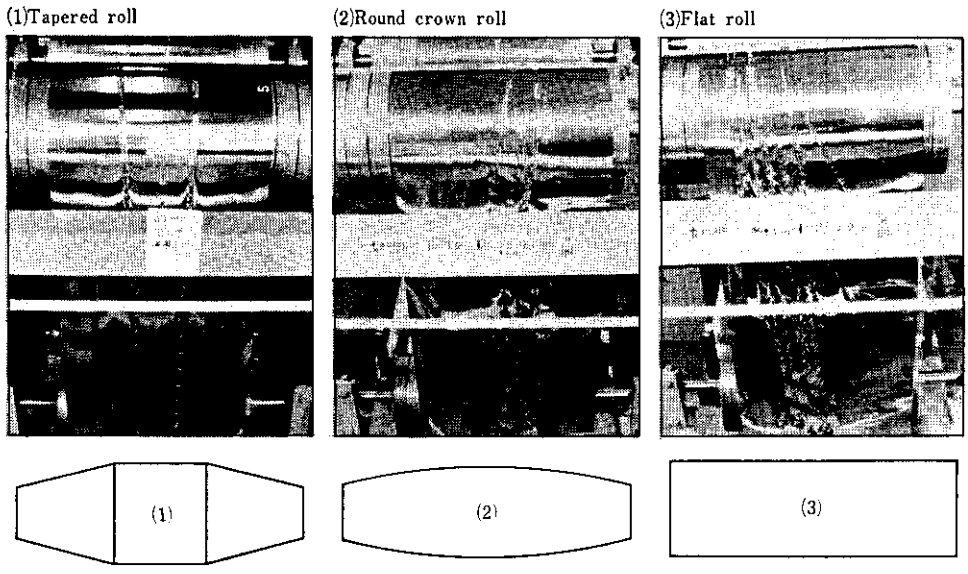

Photo 1 Appearance of buckled Al foil in experimental equipment

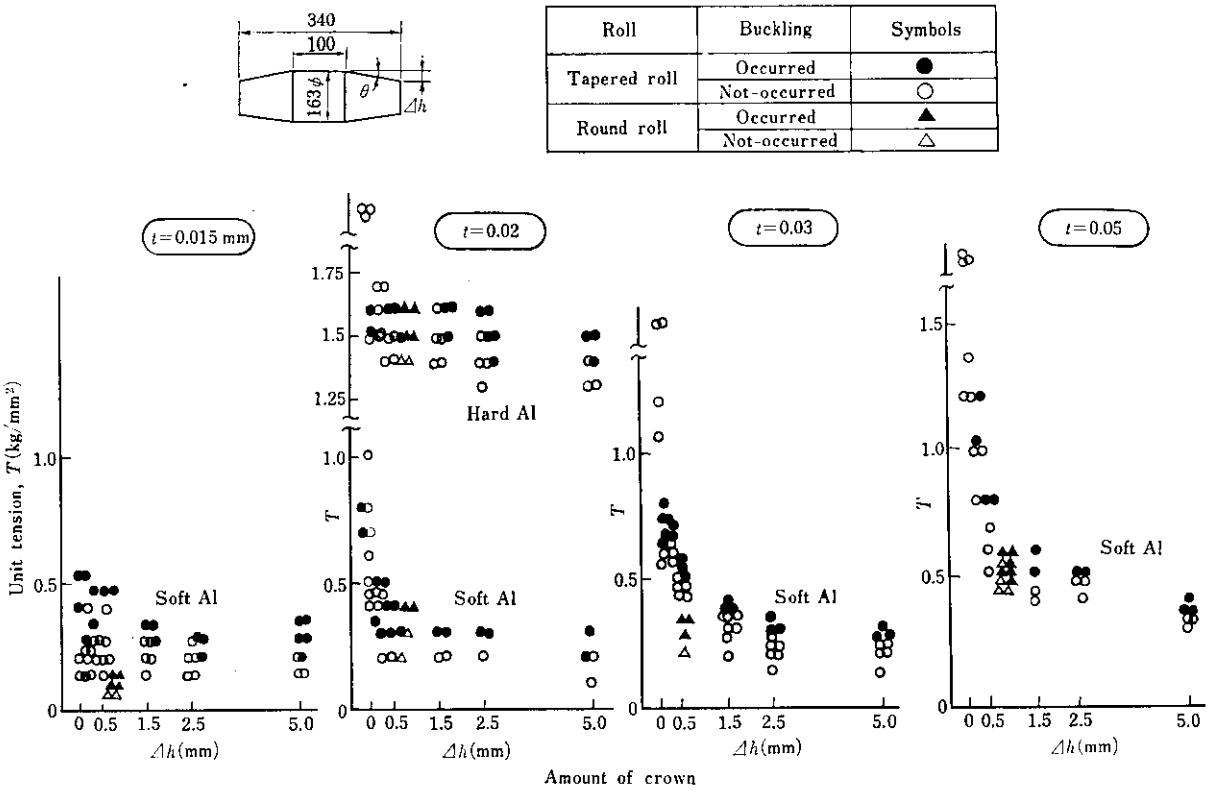

Fig. 2 Critical tension of buckling in Al foil experiment

rolls with a radius difference (Δh) of 0 to 5.0 mm between the middle and the end of rolls and round rolls of the same Δh were used for this experiment. The white circles in the figure indicate that buckling did not occur, and the black ones indicate that buckling occurred. The material tension at the boundary between the two is called the critical buckling tension (T_{cr}). Results of the experiment are summarized as follows:

(i) Buckling occurs when the material tension increases.
(ii) T_{cr} decreases with increasing Δh. The smaller the value of Δh, the greater the gradient of the Δh versus T_{cr} curve.
(iii) The larger the material thickness, the larger the value of T_{cr}.
(iv) The T_{cr} of a fully-annealed material is smaller than that of a temper-rolled material.
(v) In the case of the roll profile shown in Fig. 2, the T_{cr} of a tapered roll is larger than that of a round roll if a comparison is made with the same Δh.

The above-mentioned experimental results are in good agreement with a tendency observed in commercial lines.

3.2 Effect of Roll Profile

To find an optimum roll profile, the critical buckling tension (T_{cr}) was investigated by incorporating the rolls R_1 to R_4 shown in **Fig. 3**, the crown (Δh) of which was varied as roll A of the experimental equipment in Fig. 1. Aluminum foil 35 μm in thickness (t) and 250 mm in width (B) was used for this investigation. The rolls R_1 and R_2 are the above-mentioned round and tapered rolls, respectively. R_3 is a double tapered roll that has flat portions from about the middle of the tapered portions to the ends. R_4 is made by rounding the shoulders of the tapers of the roll R_2. R_5 is a small-diameter flat idle roll installed immediately before R_2 as an auxiliary roll, and the material is wound on R_2 after it contacts R_5. It is apparent from Fig. 3 that the T_{cr} of R_1 is smaller than that of any other roll when Δh is the same and that buckling is apt to occur most in this roll profile. Second to R_1, the T_{cr} of R_2 is the smallest, and then T_{cr} increases in the order: R_3 to R_4. It is R_5 that has the largest T_{cr} and is most effective in preventing buckling. The reason why R_3 is more effective than R_2 and buckling is less apt to occur is as follows. Because the material edges contact the flat portions of the roll ends before the material is completely fitted to the tapered portions, the taper angle of the material in contact with the roll

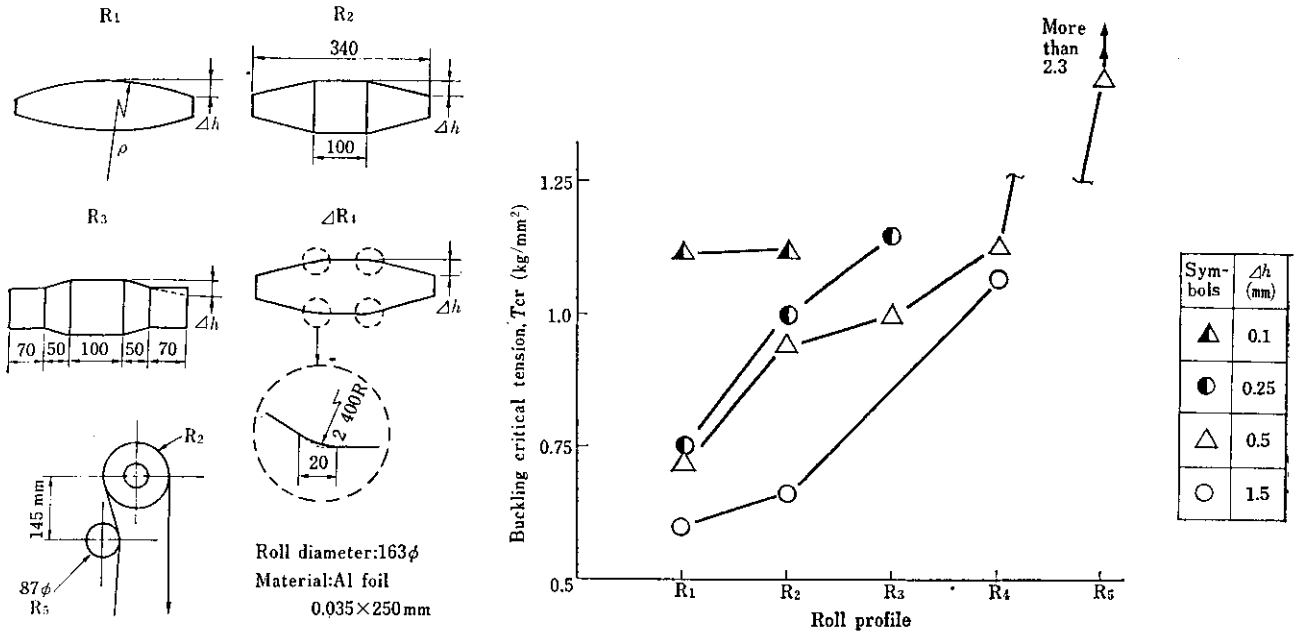

Fig. 3 Effect of roll profile on buckling critical tension (T_{cr})

is smaller than that of R_2. The reason why the rounded shoulder in R_4 control occurrence of buckling is that it can relax compressive stresses generated in these portions of the material. The roll crown develops nonuniform tension distribution in the width direction of the material, which induces compressive membrane stresses in the material. Heat buckling is considered to be caused by these compressive stresses, and buckling wrinkles are further subjected to bending and unbending by hearth rolls and show appearances with folds as shown in Photo 1. The use of R_3 and R_4 is a means of relaxing the above-mentioned compressive stresses. R_5 is effective for increasing critical buckling stresses. That is to say, the bending deflection of the material is depressed by the flat surface of the roll installed near the hearth roll. It is apparent from Fig. 3 that T_{cr} is increased by more than double by installing R_5 near R_2.

Next, an investigation was made into the effect of the position of R_5 relative to R_2 on T_{cr}. **Figure 4** shows results of this investigation. In this figure, the standard position satisfies $y_h = 145$ mm ($y_h/D_2 \fallingdotseq 0.9$, D_2 = diameter of R_2) and $x_h = 0$ mm (the center of R_5 is located on the vertical line through the point A). As shown in this figure, the larger x_h (R_5 is pushed toward R_2) and the smaller y_h (the distance between R_2 and R_5 decreases), the more T_{cr} will increase. Results of the simulation test reveal that buckling is not apt to occur if $y_h/D_2 \leq 1.5$ and $x_h/D_2 \geq -0.1$.

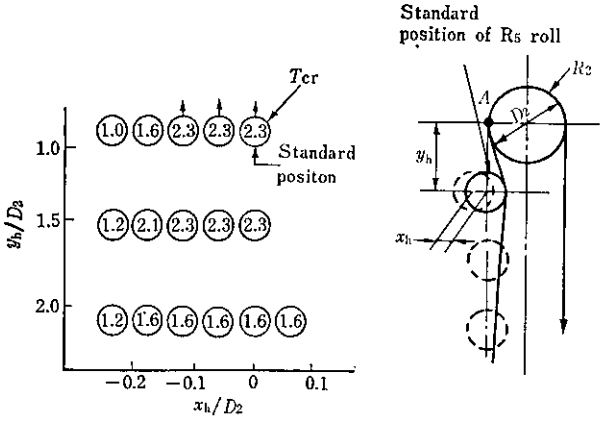

Fig. 4 Effect of position of attached R_5 on buckling critical tension (T_{cr})

4 Mechanism of Heat Buckling

Stresses generated in the strip near the hearth rolls in a continuous annealing furnace were calculated by the finite element method (FEM)[4]. **Figure 5** shows the model used for the FEM analysis. The object of the analysis is a rectangular plane 1 300 mm in length (L) from a point of contact between the strip and the hearth roll and 1 035 to 1 610 mm in width (B). The shape of elements is a triangle, the number of elements is 124 to 191, and the number of nodes is 78 to 115. The tapered roll with flat portion in the middle, shown in Fig. 5, was used as the hearth roll and the width (H) of the flat portion was varied between 230 and

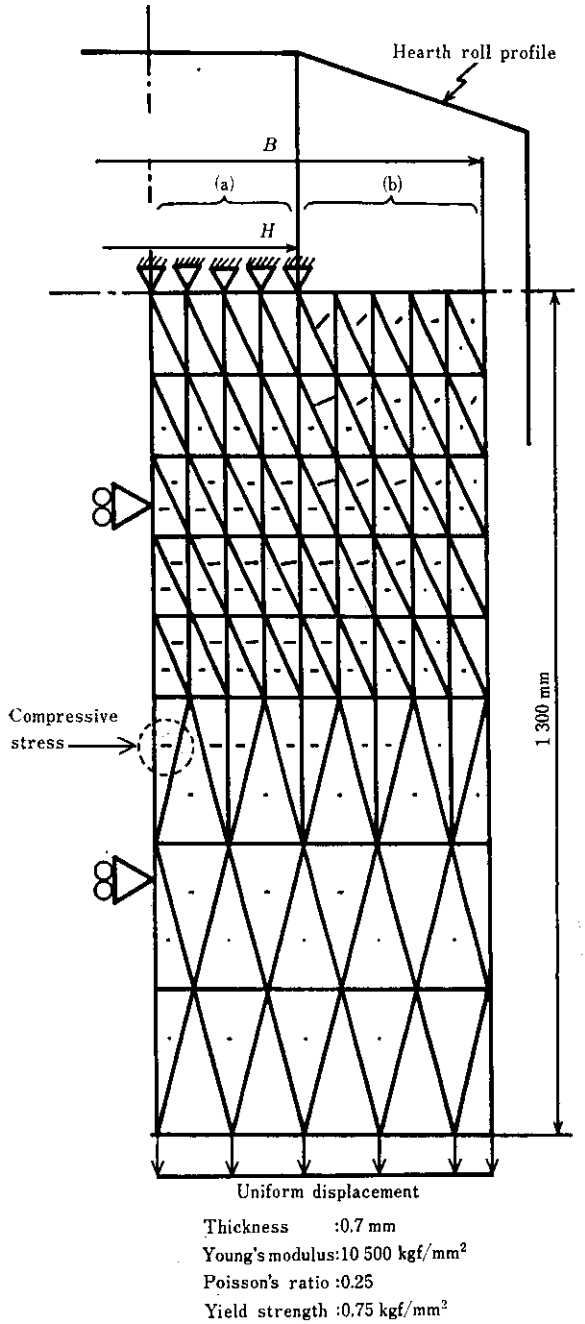

Fig. 5 Distribution of induced compressive stress calculated by finite element method (Plane stress)

920 mm. The contact of the tapered portion of the roll with the strip was not considered, and uniform displacement (U) was given to the bottom end of the strip in Y-direction by constraining the nodal displacement of the strip in contact with the flat portion of the roll both in the lateral (X) and vertical (Y) directions. Since the bending deflection of the strip was neglected and the amount of deformation was small, the stress and strain were calculated as elastic ones. The mechanical properties of pure iron at 850°C were adopted for the strip; that is, the yield strength (Y.S.) is 0.75 kgf/mm² [5], Young's modulus (E) 10 500 kgf/mm² [6], and Poisson's ratio (ν) 0.25.

Only the compressive component of σ_2 is extracted from the principal stresses σ_1 and σ_2 generated in each element and its direction and magnitude are illustrated as the vector of σ_2 in Fig. 5. This figure reveals that in the portion of the strip near the hearth roll, strong compressive stresses are generated aslant from left to right upward in an area corresponding to the shoulder of the roll where the taper begins. The type of heat buckling observed in a thin and wide strip in a commercial line can be explained well if in the portion of the strip corresponding to the shoulder, these compressive stresses cause buckling to occur at right angles with the direction of the compressive stresses and aslant with respect to the direction of strip travel and

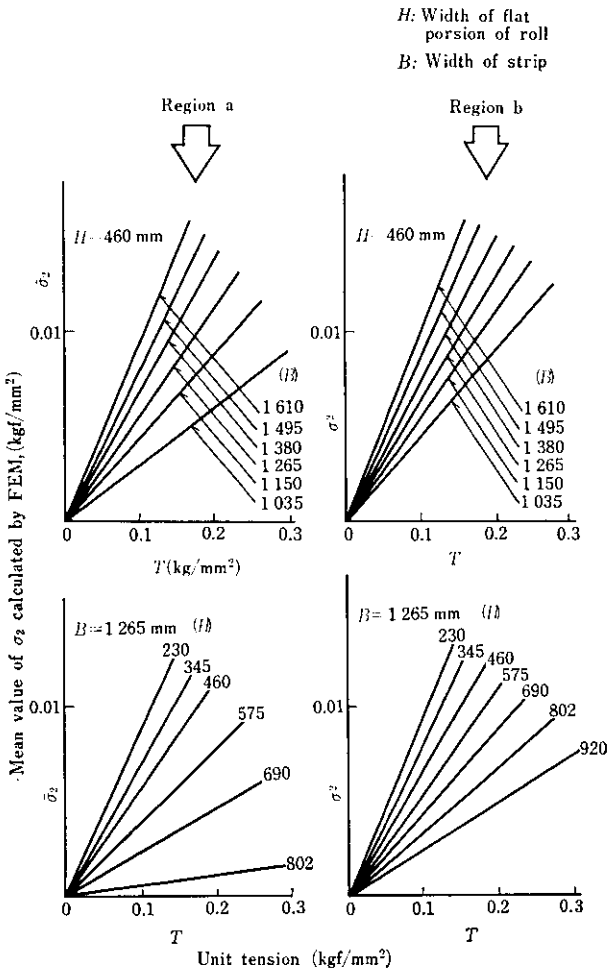

Fig. 6 Relations between unit tension (T) and mean compressive stress ($\bar{\sigma}_2$)

the strip is wound on the hearth roll in this condition. Compressive stresses at the shoulder of the taper decrease gradually as the distance of elements from the hearth roll increases. However, relatively large widthwise compressive stresses are observed in the middle of the strip. These compressive stresses in the middle may cause heat buckling to take place parallel to the direction of strip travel. Compressive stresses become very small at points distant from the point of contact with the hearth roll by the same degree as the strip width.

Figure 6 shows the calculated mean value of σ_2 ($\bar{\sigma}_2$) generated in the strip when the width (H) of the flat portion of the roll and the width (B) of the strip are varied. $\bar{\sigma}_2$ was calculated by the following equation for both the flat portion of the roll (region (a) in Fig. 5) and the tapered portion of the roll (region (b) in Fig. 5):

$$\bar{\sigma}_2 = \frac{\sum (A_i \cdot \sigma_{2i})}{\sum A_i} \quad \cdots\cdots (1)$$

i: Element number
A: Area of each element

As shown in Fig. 6, compressive membrane stresses increase with increasing material tension (T). In both regions (a) and (b), the larger the strip width (B) and the smaller the width (H) of the flat portion of the roll, the larger the increase in $\bar{\sigma}_2$ relative to the increment in tension ($d\sigma_2/dT$). This suggests that heat buckling tends to occur. The $\bar{\sigma}_2$ of region (a) is more sensitive to change in H and B than that of region (b). It is found, however, that in the same strip, the value of $\bar{\sigma}_2$ in region (b) is larger than that of $\bar{\sigma}_2$ in region (a).

Next, the buckling rigidity of regions (a) and (b) is discussed. As shown in **Fig. 7**, the three sides (I), (II) and (IV) of region (a) were regarded as single supports and the side (III) was regarded as a free support. In the case of region (b), the sides (I) and (III) were supposed to be free supports, and the sides (II) and (IV) single supports. The critical buckling stress of region (a) ($\sigma_{cr(a)}$) is given by the following equation when the buckling deflection of the strip shows a single wave with half wave length:

$$\sigma_{cr(a)} = \frac{k\pi^2 D}{H^2 t} \quad \cdots\cdots (2)$$

D: Bending rigidity, $D = Et^3/12(1 - \nu^2)$

k: The magnitude of L/H (L is the length of the sides (II) and (IV) and approximately given by the following equation.)

It is known that the larger L/H, the larger the value of k will be[7,8].

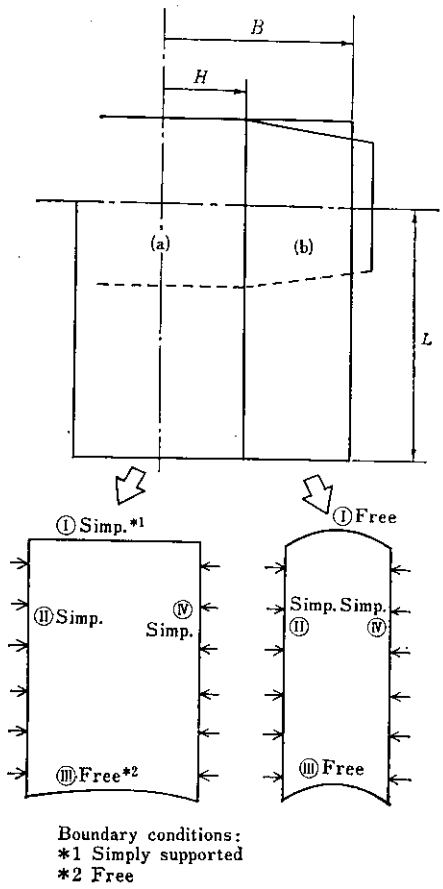

Fig. 7 Boundary conditions of buckling model of strip

$$k \fallingdotseq 0.42\left(\frac{L}{H}\right)^2 \quad \cdots\cdots (3)$$

The critical buckling stress of region (b) ($\sigma_{cr(b)}$) is given by the following equation:

$$\sigma_{cr(b)} = \frac{4(1 - \nu^2)\pi^2 \cdot D}{(B - H)^2 \cdot t} \quad \cdots\cdots (4)$$

From eqs. **(2)** and **(4)**, the ratio of $\sigma_{cr(a)}$ to $\sigma_{cr(b)}$ is expressed as follows:

$$r = \frac{\sigma_{cr(a)}}{\sigma_{cr(b)}} = \frac{0.105\{L(B - H)\}^2}{H^4(1 - \nu^2)} \quad \cdots\cdots (5)$$

If the values used for the calculation shown in Fig. 5, L of 1 300 mm, B of 1 035 to 1 600 mm and H of 460 mm, are substituted in eq. **(5)**, r becomes greater than 1, i.e., $\sigma_{cr(a)}$ is greater than $\sigma_{cr(b)}$. This shows that buckling occurs in region (b) earlier than in region (a).

The fitting of the strip over the tapered portion of the roll is taken into consideration as an index for evaluating the tendency toward buckling in region (b). If, as shown in **Fig. 8**, the area of 1/4 of the cylindrical

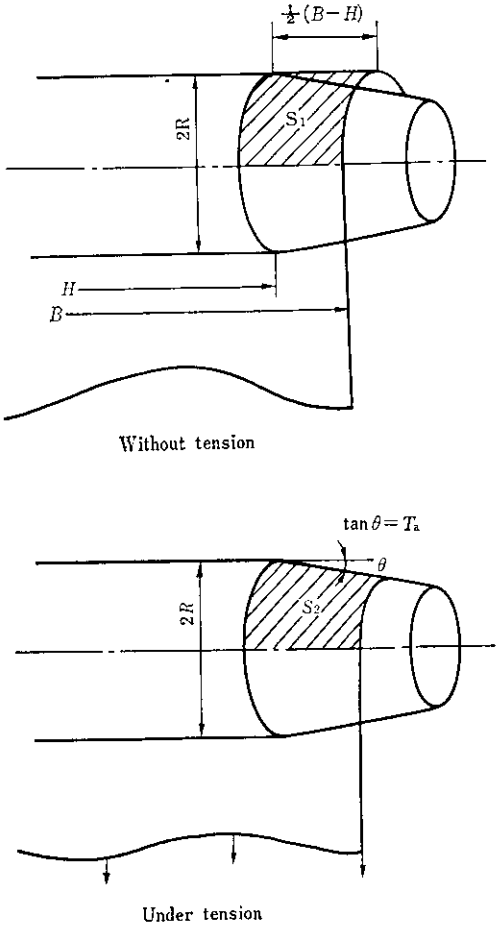

Fig. 8 Fitting ability model of the strip to tapered hearth roll surface

part of the strip is denoted by S_1 when the strip is not fitted at all over the tapered portion of the roll and it is denoted by S_2 when the strip under tension is completely fitted over the tapered portion, then S_1 is greater than S_2. The larger the remainder of $(S_1 - S_2)$, the larger the surplus area of the strip that fits over the tapered portion and heat buckling is apt to occur in this condition. Therefore, the surplus area rate (φ_S) given by the following equation is used as a new parameter indicating the tendency toward heat buckling:

$$\varphi_S = \frac{S_1 - S_2}{S_1} = \frac{(B - H)T_a}{4 \cdot R} \quad \cdots\cdots\cdots (6)$$

T_a: The roll taper given by $T_a = \tan\theta$ if the taper angle is denoted by θ

R: the radius of the hearth roll

Three parameters $d\bar{\sigma}_2/dT$, $\bar{\sigma}_{cr(b)}$ and φ_S were proposed as effects on the critical buckling tension (T_{cr}) in the above-mentioned considerations. That is to say,

(a) The larger the $d\bar{\sigma}_2/dT$ obtained by FEM analysis, the smaller the value of T_{cr}. The $d\bar{\sigma}_2/dT$ in the tapered portion is larger than that of the parallel portion.

(b) Since the $\sigma_{cr(b)}$ of the tapered portion is smaller than that of the flat portion, the former value is adopted. The smaller $\sigma_{cr(b)}$, the smaller T_{cr}.

(c) The larger the surplus area rate (φ_S) of the strip in the tapered portion, the smaller T_{cr}.

Supposing that the product of the parameters $dT/d\sigma_2$, $\sigma_{cr(b)}$ and $1/\varphi_S$ above mentioned in (a) to (c) is proportional to T_{cr} and that the proportionality constant is denoted by K, the authors obtain the following equation for evaluating T_{cr} under operating conditions:

$$T_{cr} = K \cdot \frac{R \cdot E \cdot t^2}{(B - H)^3 \cdot T_a} \cdot \frac{dT}{d\bar{\sigma}_2} \quad \cdots\cdots\cdots (7)$$

In order to confirm the validity of eq. (7), experiments were conducted in the KM-CAL[9] at the Chiba Works. An ultralow carbon (0.002%C) steel strip with 0.7 mm thickness (t) and 1 095 to 1 320 mm width (B) was treated in the continuous annealing line at a soaking temperature of 810 ± 20°C, and an investigation was made as to whether heat buckling occurs under conditions of varied strip width (B) and tension (T). **Figure 9** shows results of this investigation. The black circles in the figure shows the conditions under which heat buckling occurred, and the white ones the conditions under which heat buckling did not occur. This figure also contains the critical buckling tension calculated by eq. (7) at $K = 4.04 \times 10^{-3}$. The region above this T_{cr} curve shows the range where heat buckling occurs. The results calculated by eq. (7) are in considerably good agreement with the experimental results in the commercial line. Therefore, this

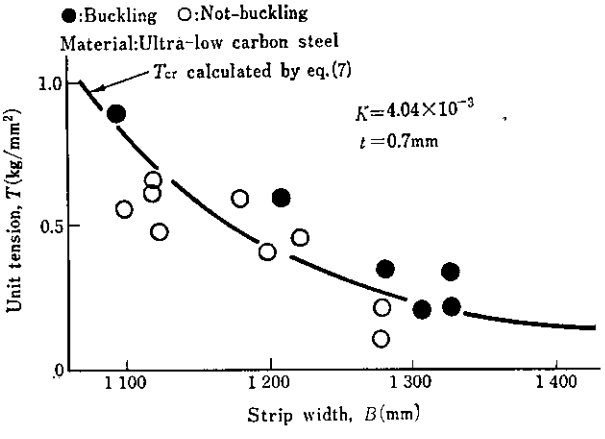

Fig. 9 Comparison between actual buckling critical tension and calculated curve by eq. (7)

equation can be used for predicting whether heat buckling will occur or not under operating conditions.

5 Mechanism of Correcting Snaking by Hearth Roll

It is well known[10] that when a strip material wound on the roll at an angle of β with the direction of roll rotation, as shown in **Fig. 10**, rotates together with the roll, the material shifts toward the middle as indicated by the broken lines and snaking is corrected. Therefore, the material does not shift in the width direction when $\beta = 0$. If the amount of shift of the material toward the middle of the roll width per roll rotation is denoted by Δx, Δx is geometrically approximated by the following equation:

$$\Delta x \fallingdotseq 2\pi R \tan \beta \fallingdotseq 2\pi R\beta \quad \cdots\cdots\cdots\cdots (8)$$

If a strip material wound on the tapered portion of the roll at β of 0 is developed in a plane, its configuration is as shown by the solid lines in **Fig. 11**. If the roll taper angle is θ, the peripheral velocity of the roll is the unit angular velocity, and the material width is the unit width, then the difference (Δv) between the peripheral velocities v_a and v_b of the two sides a and b of the material is given by the following equation:

$$\Delta v = \tan \theta \fallingdotseq \theta \quad \cdots\cdots\cdots\cdots\cdots\cdots (9)$$

Due to this velocity difference, the material is given the counter-clockwise moment shown in Fig. 11. It is supposed that this moment causes the material to rotate at an angle of β with the direction of roll rotation, as shown in the figure. That is to say, Δv is determined depending on θ, and Δv generates the above-mentioned moment in the material. This moment produces the condition of $\beta > 0$ and the material shifts as shown in Fig. 10, with the result that snaking is corrected. Therefore, the relationship between θ and β was presumed by the following equation:

$$\beta \propto \theta \quad \cdots\cdots\cdots\cdots\cdots\cdots\cdots\cdots (10)$$

If the proportionality constant of eq. **(10)** is denoted by α, the following equation is obtained by substituting α into eq. **(8)**:

$$\Delta x = \alpha \cdot 2\pi R \cdot \theta \quad \cdots\cdots\cdots\cdots\cdots\cdots (11)$$

Equation **(11)** is rearranged as follows if it is supposed that the material shifting is governed by the degree of the mean gradient (θ_m) in roll portion corresponding to the whole material width when the material is in contact with both the flat portion and the tapered portion of the roll or when θ changes gradually in the width direction as in a round roll:

$$\Delta x = \alpha \cdot 2\pi R \cdot \theta_m = \alpha \cdot 2\pi R \cdot \frac{1}{B}\int_{x_0}^{x_1} \theta \, dx \quad \cdots\cdots (12)$$

B: Material width

x_0, x_1: X-coordinates of both edges of the material when the middle of the roll width is zero

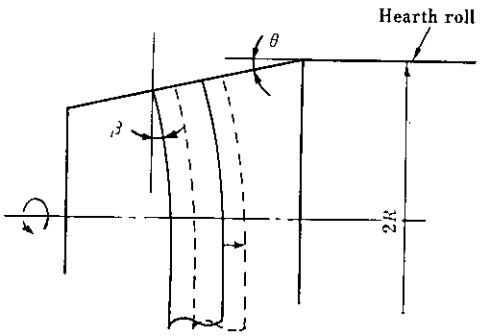

Fig. 10 Self-centering motion of the strip wound to tapered portion of roll with angle

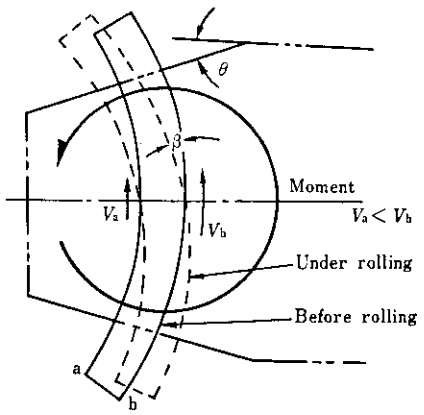

Fig. 11 Moment on the strip wound to tapered portion of roll

To confirm the validity of eq. **(12)**, a rubber band with t of 1 mm and B of 200 mm was wound between rolls A and B of the experimental equipment shown in Fig. 1 and the amount of shift of the material in the width direction was measured by rotating the rolls. Rolls of various profiles were used as roll A and a flat roll was used as roll B. The sizes of material width and roll diameter correspond to 1/5 of those of the commercial-scale line. With the amount of crown (Δh) set constant at 0.5 mm, changes in Δx per roll

rotation were measured by varying the position where the material is placed. Three types of roll were used for this experiment. **Figure 12** shows results of this experiment. In this figure, the abscissa is the coordinate of the middle of the material width (M_c) when the middle of the roll width is taken as zero. The ordinate is Δx; when this value is large, the ability to correct snaking is great. As shown in this figure, Δx equals 0 when M_c is 0, that is, the material is placed in the middle of the roll width. When the material shifts from the middle of the roll width and $|M_c|$ becomes larger than zero, Δx increases and the ability to correct snaking increases. This figure contains calculated values of Δx when α is 0.349 in eq. **(12)**. The points where the curves of calculated Δx are broken indicate that the edges of the material are placed at the boundaries between the tapered and flat portions of the roll. As shown in this figure, there is a relatively good agreement between the calculated and observed values. This demonstrates that the evaluation of the ability to correct snaking by eq. **(12)** is proper. When the effect of the roll profile on Δx is examined, it is found that, at the same M_c, the Δx of the tapered roll is larger than that of any other rolls. Second to the tapered roll, the round roll shows the larger value and the double tapered roll has the worst ability to correct snaking.

Equation **(12)** expresses the amount of shift of the material per roll rotation depending on the position where the material is placed; therefore, the total amount of shift of the material (S_x) at a certain number of roll rotations (N) can be calculated by addition.

Figure 13 (a) and (b) show calculated and experimental values of S_x and N, respectively, for the round and tapered rolls, when the material is set so that its edge in width direction with the end of the roll ($M_c = -70$) in the initial stage and then the roll is rotated. The amount of taper Δh was set at three different levels: 0.1, 0.25 and 0.5 mm. As is apparent from the figure, the experimental values are in good agreement with the calculated values. When Δh is large, the number of roll rotations (N) until the material shifts to the middle of the roll width ($S_x = 70$) is small, that is, the strip can return rapidly to the middle of the roll width. Furthermore, it is found that when Δh is the same, the tapered roll has a greater ability to correct snaking than the round roll.

An investigation was made into the effect of the auxiliary roll R_3 shown in Fig. 3 on the snaking behavior of the material. Results of this investigation

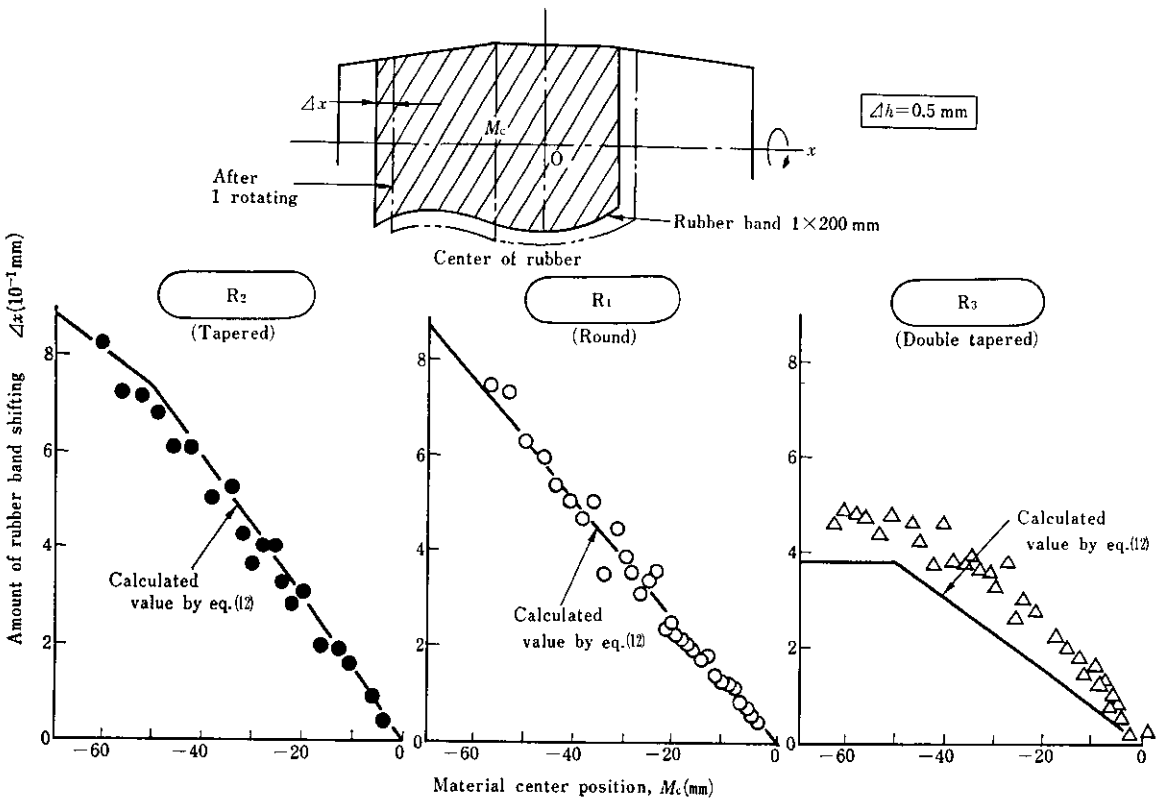

Fig. 12 Amount of rubber band shifting per one roll rotation according to position settled

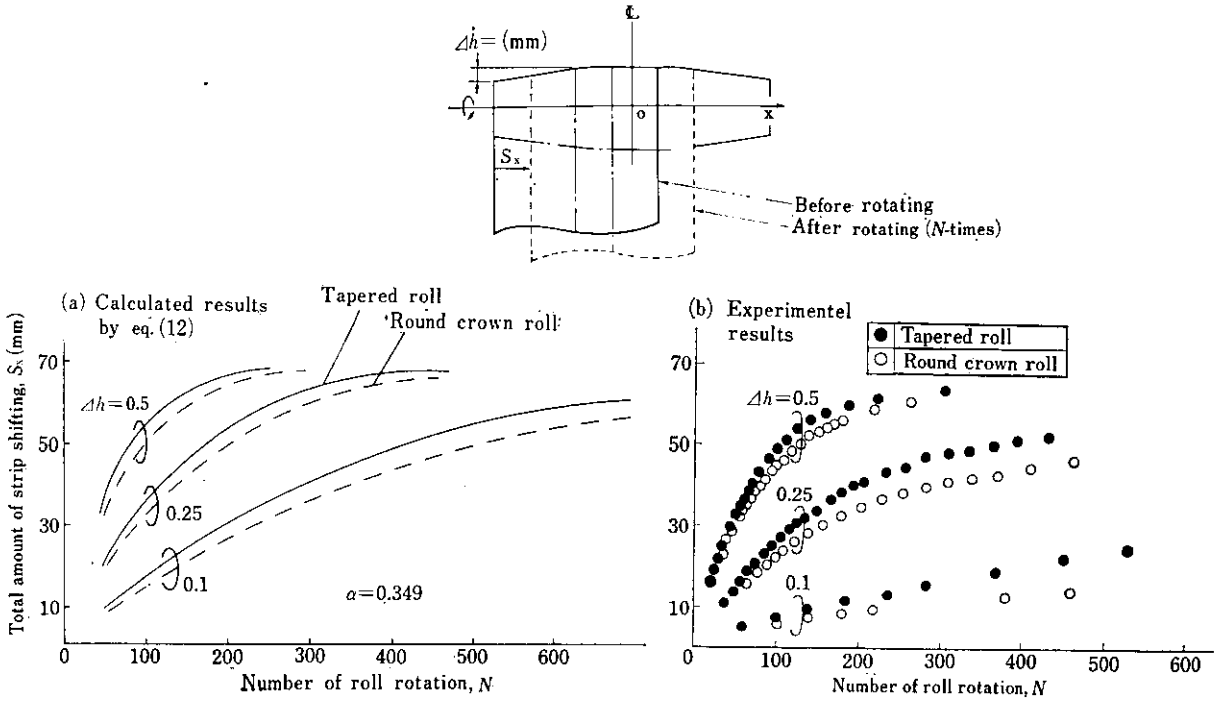

Fig. 13 Relations between number of roll rotation (N) and total amount of strip shifting (S_x)

is described in the following. The roll R_5 was installed in the standard position shown in Fig. 4 and the angle (γ) between the axes of R_5 and R_2, indicated in the plan view shown in **Fig. 14**, was changed. The relationship between S_x and N was obtained by setting the material in the initial stage in such a way that

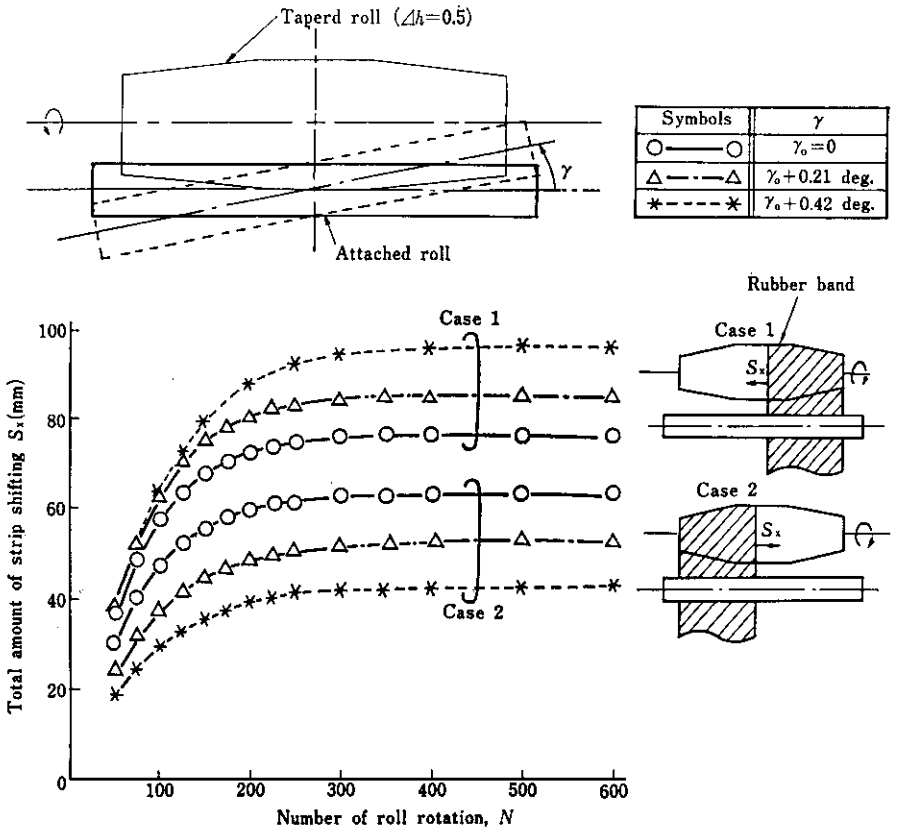

Fig. 14 Effect of attached roll on weaving controll ability of hearth roll

hte material edge coincides with the right end of the roll R_2 in Case 1 and to the left end in Case 2. Figure 14 shows the relationship between N and S_x at various γ-values: $\gamma_0(\fallingdotseq 0)$, $\gamma_0 + 0.21°$ and $\gamma_0 + 0.42°$. The S_x-N relationship in Cases 1 and 2 should be the same if the condition for the lateral symmetry is completely satisfied at $\gamma = 0$. This condition is virtually satisfied when $\gamma = \gamma_0$. When γ is increased, the difference between S_x of Case 1 and S_x of Case 2 increases and the material tends to shift to the wider side in an angle formed by the axis of R_2 and the axis of R_5. However, when N is 400 or over, there is a good balance between the snaking correcting ability of R_2 and the snaking promoting ability of R_5 due to improper setting ($\gamma \neq 0$) and S_x becomes constant. The S_x, when the middle of the material width corresponds with that of the roll width, is 70 mm in this experiment, and a deviation from S_x of 70 mm (ΔS_x) represents the amount of shift from the middle of the roll width. When γ is the same, the material position at a maximum of S_x is the same in Cases 1 and 2 and the amount of shift from the middle is also expressed by ΔS_x. From Fig. 14, ΔS_x is approximately 10 mm/0.21 deg when a roll R_2 with Δh of 0.5 mm is used. This means that, when the roll R_5 is installed, it is necessary to rigidly control its parallelism with the hearth roll. If this parallelism is sufficiently satisfied, the roll R_5 does not hinder the function of the hearth roll for correcting snaking, as will be understood from a comparison between the case of $\Delta h = 0.5$ mm shown in Fig. 13 and the case of $\gamma_0 \fallingdotseq 0$ in Fig. 14.

6 Conclusions

To p event the heat buckling and snaking of a strip in the heating and soaking zones of a continuous annealing furnace, a simulation test using aluminum foil and a rubber band, theoretical analysis by the FEM and experiments in a commercial line were conducted and the following results were obtained:

(1) The crown of the hearth roll makes the strip tension nonuniform and compressive membrane stresses (σ_2) generated by this nonuniform tension cause heat buckling.

(2) Buckling occurs when the material tension exceeds a certain critical value (T_{cr}). T_{cr} decreases with increasing amount of roll crown, amount of taper (T_a) and material width (B) and decreasing material thickness (t), yield stress of the material and width (H) of the flat portion of the tapered roll.

(3) The following equation was introduced as a formula for determining T_{cr} from theory and experiments:

$$T_{cr} = K \frac{Et^2R}{(B-H)^3 T_a} \cdot \frac{dT}{d\bar{\sigma}_2}$$

(4) The roll profile has a great effect on T_{cr}. A tapered roll, or a roll with rounded shoulders at taper, or a double-taper roll is less susceptible to heat buckling than a round roll.

(5) A substantial improvement in T_{cr} is obtained by installing auxiliary cylindrical rolls near the hearth roll to flatten the strip.

(6) The following proposed equation expresses the snaking characteristics that are determined by the roll profile and the position where the strip is placed:

$$\Delta x = \alpha \cdot 2\pi R \frac{1}{B} \int_{x_0}^{x_1} \theta \, dx$$

This equation permits a quantitative evaluation of the snaking correcting capacity of the hearth roll profile.

References

1) T. Hira, H. Abe et al.: *Tetsu-to-Hagané*, under contribution
2) T. Fukushima: The 88th Nishiyama Seminar
3) T. Matoba, I. Aoki: *The Proceedings of the 32th Japanese Joint Conference for Technology of Plasticity*, (1981), p. 579
4) Y. Yamada: Sosei Nendansei (Plasticity Visco-elasticity), Baifu-kan, p. 180 (1972)
5) S. Sakui, T. Sakai: *Journal of the Japan Institute of Metals*, **40** (1976), p. 263
6) C.W. Andrews: *Metal Progress*, **7** (1950), p. 85
7) S. Timoshenko: Theory of Elastic Stability, Mcgraw-hill Book Company, (1936), p. 324
8) C. R. C. Japan: Handbook of Structural Stability, Corona (1971)
9) F. Yanagishima, Y. Shimoyama et al.: *Kawasaki Steel Giho* **13** (1981) 2, p. 1
10) S. Inada: Study of Mechanism, Asakura-shoten